Low-frequency Synthetic Aperture Radar Imaging of Complex Scenes using Numerical Electromagnetic Analysis

Michael Simcoe[a], Raviraj Adve[a], Joseph Schneible[b], Michael Wicks[c]

[a] University of Toronto
Department of Electrical and Computer Engineering
10 King's College Road
Toronto, ON M5S 3G4 Canada
[b] Stiefvater Consultants
10002 Hillside Terrace
Marcy, NY 13403, USA
[c] Air Force Research Laboratory (AFRL/SNRT)
26 Electronics Parkway
Rome, NY 13244, USA

Abstract-This work develops the high-fidelity simulation capability for low-frequency synthetic aperture radar (SAR) imaging of complex scenes including both metal and dielectric regions. The simulation is based on a Method of Moments (MOM) numerical electromagnetic analysis of scenes where metal targets are obscured by foliage modeled as dielectric. The ability to accurately model the interaction of foliage and target is crucial for an accurate simulation. Example scenes for isolated metal targets are provided in addition to scenes with combined metal and dielectric targets. As expected, the effect of the surrounding foliage is shown to have a significant impact on the reconstructed target image. This approach will be useful in low-frequency SAR applications for the prediction of target signatures under various conditions of concealment.

I. INTRODUCTION

Low-frequency synthetic aperture radar (SAR), operating mainly in the VHF and UHF bands, can potentially locate and image strategic targets concealed under trees. This general approach where low-frequency radar signals are used for the location or imaging of targets under trees has been termed foliage penetrating (FOPEN) radar. The practical development of FOPEN requires extensive research into almost all aspects of radar including antennas, platforms, signal processing, target recognition, etc. In other research areas, simulations play an important role to develop, test and validate new concepts quickly and cheaply. An excellent example of this is Space Time Adaptive Processing (STAP) where realistic models are available for targets, clutter and interference [1]. In STAP simulations, the return signal is modeled as a sum of the target and foliage signals.

Unfortunately, in the FOPEN case, the target signals interact with the surrounding foliage. The modeling of the return signal as the sum of target and interference ignores this interaction. The classical simulation techniques are therefore not valid. The actual return signal is the solution to Maxwell's equations for the given radar scene which accounts for the signals returned by the target, the foliage and any possible interaction between target and foliage. There is no closed form solution to Maxwell's equations in this case and so a numerical electromagnetic analysis is required.

Here, to obtain realistic simulations that capture all the necessary information, a complete numerical solution to the radar scene is performed using the Method of Moments (MOM) [2]. The MOM numerically solves the integral form of Maxwell's equations. The solution leads to the surface electric (and magnetic in the case of dielectrics) currents on the bodies being analyzed. However, using the MOM poses significant challenges. In general, MOM techniques subdivide the analysis region with about 10 subdivisions for each wavelength λ or 100 subdivisions per λ^2. This problem is worsened by the fact that any FOPEN radar scene must include dielectrics. The surface of dielectrics must be discretized in terms of the wavelength within the dielectric, $\lambda_d = \lambda / \sqrt{\varepsilon_r}$, where ε_r is the relative permittivity of the dielectric. Since a practical FOPEN radar scene may cover several hundred wavelengths the total number of unknowns could be in the thousands or hundreds of thousands. Another major challenge is that each frequency in the broadband UHF/VHF frequency range used for FOPEN must be independently analyzed, worsening an already difficult problem.

This paper uses an extremely efficient MOM implementation based on coarse discretizations with complex basis functions [3]. The implementation uses only 20 unknowns per λ^2 and is available as a commercial MOM numerical analysis package, WIPL-D [4]. This package is used for a broadband frequency domain analysis of the SAR scene of interest. The data generation scheme is combined with SAR signal processing to generate some test results.

Section II describes the SAR-MOM model, including the approach taken to merge the electromagnetic analysis with the signal processing. The focus is on spotlight mode SAR. Section III presents several SAR examples of interest. Finally, section IV presents a discussion of the proposed approach and some conclusions.

II. SIMULATING SAR USING THE METHOD OF MOMENTS

A. Method of Moments SAR Model

This work simulates spotlight mode synthetic aperture radar, a particular form of SAR. We begin with a review of the operation of spotlight mode SAR. This review, based upon the description provided in [5], also serves to introduce the notation used in this paper.

The general spotlight mode synthetic aperture radar (SAR) geometry is shown in Figure 1a. The box shown centered at the origin is the spotlighted target region (STR). It has dimensions of $2X_o$ and $2Y_o$ in the *x*- and *y*-direction respectively. The synthetic aperture that corresponds to the aircraft flight path is symmetrical about the STR and has a total length of $2L$. The synthetic aperture is located at an elevation Z and at a distance X' in the x'-direction away from the center of the STR.

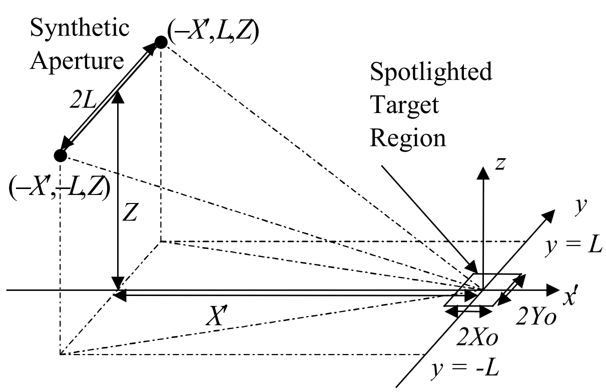

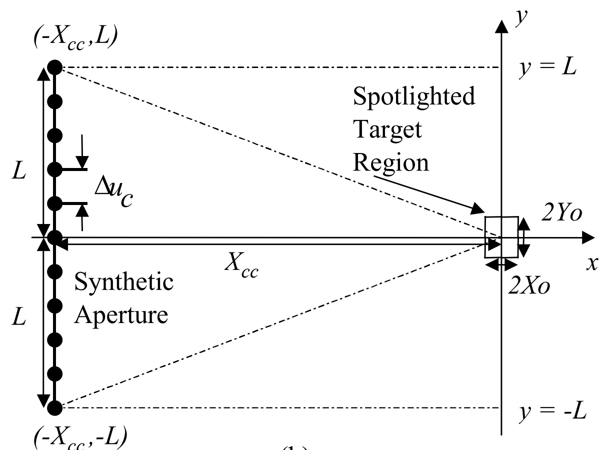

Figure 1: (a) Physical SAR geometry; (b) reduced two-dimensional SAR geometry.

As the aircraft flies along the synthetic aperture flight path, it transmits radar pulses into the STR at regularly spaced intervals (aperture points) and collects the reflected pulses from objects located in the scene. The aircraft antenna array is steered (electronically or mechanically) to always point at the STR. A linear FM pulse is used as the radar transmit signal and is given by

$$p(t) = \exp\left[j\left(\beta t + \alpha t^2\right)\right] \quad 0 \le t \le T_p, \tag{1}$$

where T_p is the pulse width and the parameters α and β are determined according to the required pulse bandwidth between some minimum frequency point f_{min} and maximum frequency point f_{max}. The spacing between aperture points (pulse transmit locations) is denoted Δu_c and is given by

$$\Delta u_c \leq X_{cc} \lambda_{\min} / (4 Y_o) , \tag{2}$$

where $\lambda_{\min} = c/f_{\max}$. The data collected from the reflected pulses along the synthetic aperture can then be used to form an image giving information about the location and geometry of targets within the STR.

Since the distance (and hence the phase shift) in the x'- and z- direction to the center of the STR are fixed, the parameters X' and Z can be combined into a total distance

$$X_{cc} = \sqrt{\left(X'^2 + Z^2\right)}, \tag{3}$$

and a corresponding cumulative phase shift to the center of the STR. This term is the slant range to the center of the target region. Combining these parameters eliminates one of the variables producing the reduced geometry shown in Figure 1b, to simplify the subsequent processing. Similarly, in the subsequent analysis discussion, the range variable x refers to the combined slant range variable $x = \sqrt{\left(x'^2 + Z^2\right)}$.

B. Linear system approach

As with all MOM numerical analysis, WIPL-D analyzes stationary scenes in the frequency domain. However, SAR is a time-domain operation with a moving aircraft. To bridge these two domains, the excitation transmit pulse spectrum $P(f)$ is multiplied with the frequency response for the scene for each particular aperture point along the synthetic aperture. Let $s(t)$ denote the received time domain signal at a particular aperture point and $S(f)$ the corresponding frequency domain signal. Also let $W(f)$ denote the frequency response of the scene, obtained using WIPL-D, at that same aperture point. Then, for that particular aperture point the received signal, at frequency f, is given by

$$S(f) = P(f) W(f) \tag{4}$$

The resulting time-domain signal, $s(t)$, at that aperture point is given by the inverse Fourier transform of $S(f)$.

The approach used here may be thought of in terms of a linear system. The frequency response obtained from WIPL-D acts as the impulse response of the system. The transmitted pulse acts as the input to the system and the received signal is output. Therefore the following relation holds

$$s(t) = p(t) * w(t) \xleftrightarrow{F} S(f) = P(f) W(f) \tag{5}$$

For each aperture point at a particular (r, φ, θ), a monostatic excitation from that aperture point direction is performed and the scattered electric field $E(r, \phi, \theta)$ at that aperture point is obtained. For each frequency point f_i in the pulse bandwidth from f_{min} to f_{max}, the calculated $E(r, \phi, \theta)$ acts as the $W(f)$ for that particular aperture point. The required time domain data can then be obtained using an inverse Fourier transform. In the implementation, the frequency axis is discretized and the electromagnetic analysis is carried out at each frequency within the frequency band of interest.

C. Discrete Fourier Transform and MOM Timing Issues

To implement this approach, the WIPL-D spectrum $W(f)$ is obtained by performing discrete simulations at a frequency spacing of Δf over the pulse bandwidth from f_{min} to f_{max}. This frequency spacing Δf is important since the total time window that can be supported following the inverse discrete Fourier transform (IDFT) is

$$T_{wind} = 1 / \Delta f \ . \tag{6}$$

All of the reflected pulses from the STR must fall within a single time window. This dictates the dimensions X_o and Y_o for the STR as well as the synthetic aperture length L that can be supported. Specifically, the minimum distance from the synthetic aperture to a point in the STR is given by

$$R_{\min} = (X_{cc} - X_o), \tag{7}$$

which is the distance from the closest point of approach, located at $y = 0$ on the synthetic aperture, to the closest edge of the STR. The maximum distance from the synthetic aperture to a point in the STR is given by

$$R_{\max} = \sqrt{((X_{cc} + X_o)^2 + (Y_o + L)^2)}, \tag{8}$$

which is the distance from an end point, located at $y=\pm L$ on the synthetic aperture, to the furthest corner of the STR. The minimum and maximum time for pulses to return from the STR are

$$T_{\min} = 2R_{\min} / c \tag{9}$$

$$T_{\max} = 2R_{\max} / c + T_p. \tag{10}$$

Hence, the following time relationship must be satisfied

$$(T_{\max} - T_{\min}) \leq T_{wind}, \tag{11}$$

or equivalently

$$2(R_{\max} - R_{\min}) / c \leq T_{wind} - T_p. \tag{12}$$

The IDFT is taken on the frequency domain signal *S(f)* to obtain the time domain signal *s(t)* at each aperture point. The backprojection spotlight SAR reconstruction algorithm available in [5] is then applied to the received signal along the aperture. Other issues relating to the sequencing of the time series data can be found in [7].

III. EXAMPLE SAR IMAGES

This section provides example results for SAR images of an STR consisting of isolated metal targets and combined metal and dielectric targets to simulate basic FOPEN type scenery. Simulations with the incident and received field both polarized along ϕ or θ are denoted $E_{\varphi\varphi}$ and $E_{\theta\theta}$ respectively.

A. Isolated metal target: T80 tank

The first target is the tank model shown in Figure 2, the dimensions of which are approximately those of a T80 series tank. The model was deliberately kept simple in order to reduce the number of unknowns and demonstrate the basic principle of operation. The SAR dimensions are $X'=Z=500m$, $X_{cc}=707.1m$, $X_0=Y_0=20m$ and $L=182m$ (corresponding to approximately a $\pm 20°$ angular range in ϕ about the STR). The frequency spacing is Δf = 1MHz and the pulse width is $T_p = 0.5\mu\sec$. Changing the frequency spacing or pulse width can accommodate other SAR dimensions. The simulated bandwidth is 250MHz between 100MHz-350MHz. The orientation of the tank for the WIPL-D simulation is shown in Figure 2. Note from the SAR dimensions provided that the synthetic aperture is positioned approximately at a $45°$ angle to the target region. Hence, the tank is seen from a perspective similar to that shown on the left in Figure 2, but from a distance of about 700 meters. The resulting φ and θ polarized backprojection spotlight SAR reconstructions are shown in Figure 3.

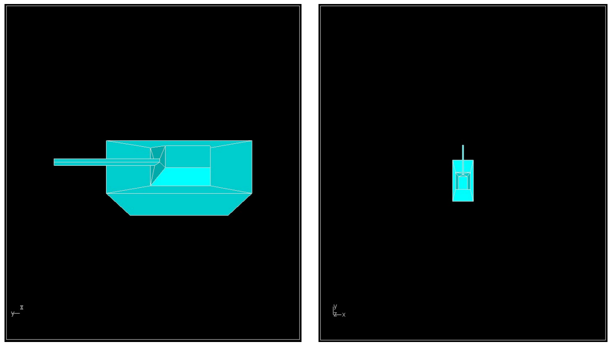

Tank Dimensions	
Chassis Length:	*7m*
Chassis Width:	*3.6m*
Turret Width:	*2.6m*
Barrel Length:	*5.5m*
Chassis Height:	*1.5m*
Total Height:	*2.2m*

Figure 2: T80 tank WIPL geometry.

The φ polarized reconstruction in Figure 3a shows the side of the tank chassis, the side of the tank turret, and an outline of the tank barrel. The features appear at the correct range location and with the correct approximate geometry in the cross-range. The reconstruction shows the strongest reflection from the side of the turret since its face is oriented upwards approximately towards the synthetic aperture producing the dominant reflection from this part of the tank. In the θ polarized reconstruction shown in Figure 3b the trailing edge of the tank chassis also appears. An explanation for the appearance of this edge is that the θ polarization induces a surface wave that diffracts off the trailing edge as observed in radar cross section analysis [6]. The location and dimensions indicated by these features are again correct. Combining the information obtained from both polarizations provides significant details about the tank location and geometry.

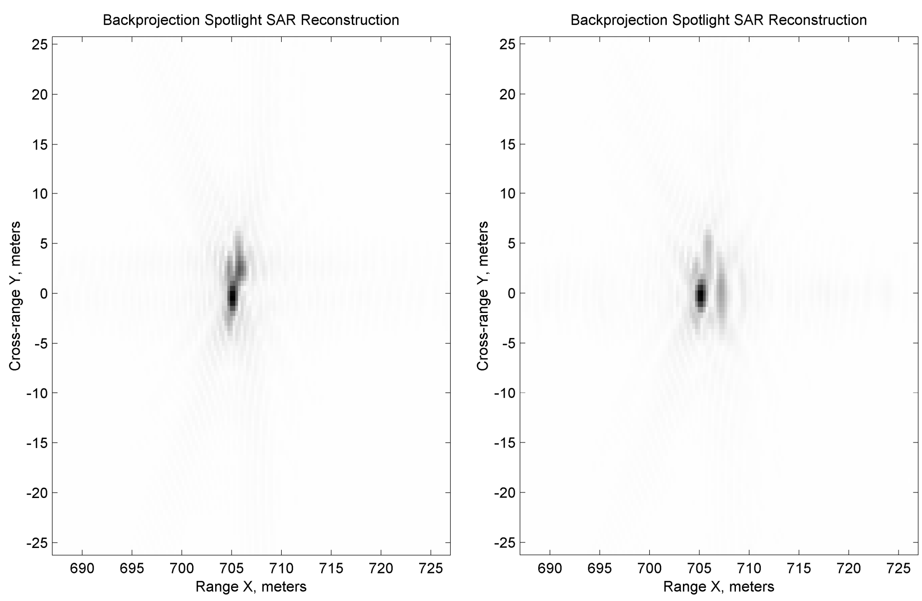

Figure 3: T80 tank backprojection spotlight SAR reconstruction. (a) $E_{\varphi\varphi}$ (b) $E_{\theta\theta}$.

B. Combined metal and dielectric targets: T80 tank and dielectric tree

This target scene contains the T80 tank and a simple tree model as shown in Figure 4. As with the tank, to reduce the number of unknowns the tree model has been kept basic: it is simply modeled as two different dielectric regions and it has no distinct branches. The dimensions and permittivity assignments for the tree are also given in Figure 4.

Its purpose is to demonstrate the effect of a general dielectric tree object on the reconstruction. The tree has been positioned directly in front of the side of the tank to obscure the view of the tank from the synthetic aperture position. The SAR dimensions, frequency spacing and pulse width have been kept the same as the previous isolated T80 simulation. The bandwidth is 230MHz from 100MHz-330MHz.

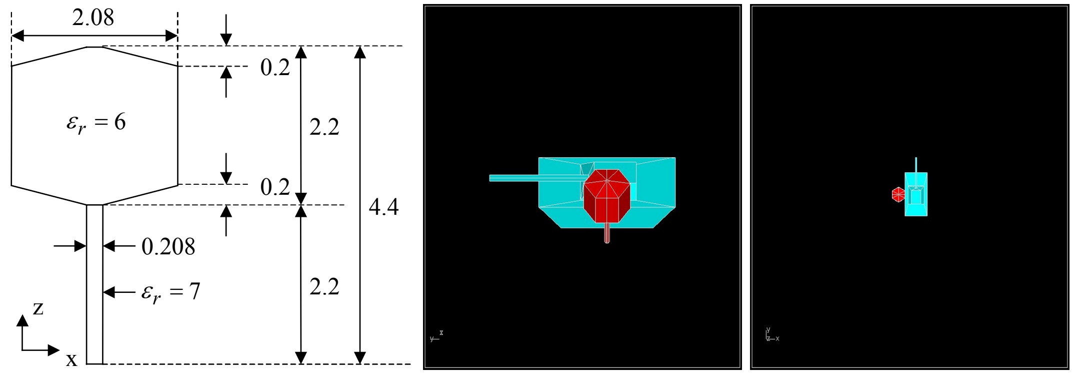

Figure 4: T80 tank and dielectric tree WIPL geometry.

The backprojection spotlight SAR reconstruction for the geometry of Figure 4 is shown in Figure 5b. For reference purposes, the backprojection spotlight SAR reconstruction for the isolated T80 tank is shown in Figure 5a. Comparing Figure 5a and Figure 5b, the SAR reconstructed image still shows the barrel outline and a portion of the side of the tank chassis near the front and rear of the tank. However, the side of the tank turret is missing. That is, the part of the tank the tree is directly blocking from the synthetic aperture view is gone. The dark area of the side of the turret appears to be shifted back in the image. An explanation for this is that the dielectric tree body introduces an additional phase lag in the signal incident upon and reflected from the turret making it appear further away in the reconstruction. Further analysis of scenes such as this involving metal targets obscured by general dielectric objects such as trees can be accomplished using this approach.

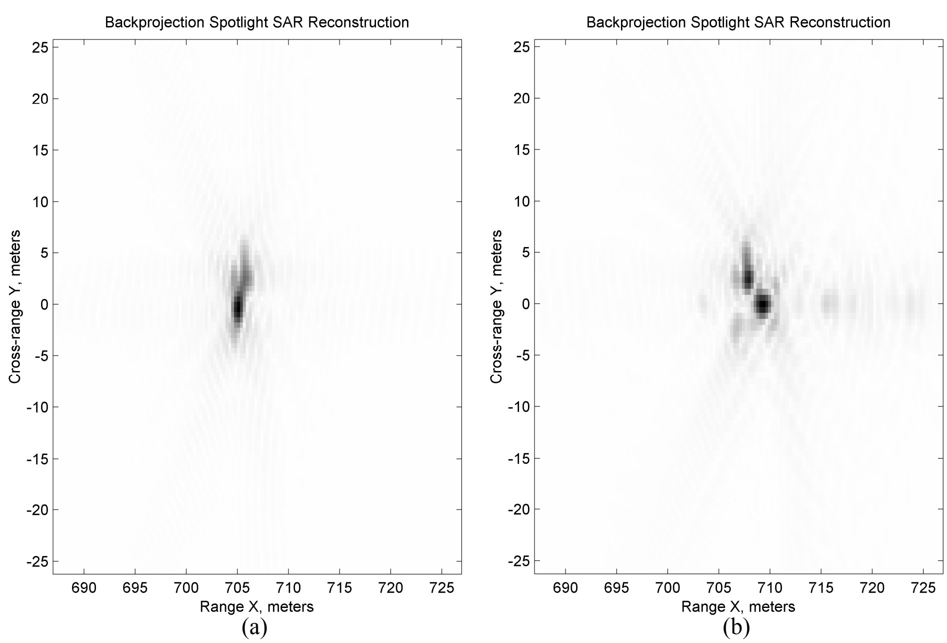

Figure 5: Backprojection spotlight SAR $E_{\varphi\varphi}$ reconstruction. (a) Isolated T80 tank; (b) T80 tank and dielectric tree.

C. A practical FOPEN scene

The target scene shown in Figure 6 represents a more practical FOPEN type situation. The tree model is now comprised of a main trunk and individual branches since in a practical FOPEN situation most of the scattering occurs from these features. Also included is a dielectric ground plane since the effect of ground bounce on the reconstructed image is significant. The trees have a height of 6m and the ground plane is 20m by 20m. The tree and ground are both assigned a permittivity of $\varepsilon_r = 7$ and a conductivity of $\sigma = 0.01$ S/m, although both of these values can be readily altered to suit the SAR scene being investigated. The SAR dimensions are $X' = Z = 40m$, $X_{cc} = 56.6m$, $X_0 = Y_0 = 12m$ and $L = 14.6m$ (still corresponding to approximately a $\pm 20°$ angular range in ϕ about the STR). The frequency spacing is $\Delta f = 4$MHz and the pulse width is $T_p = 0.05 \mu \sec$. The synthetic aperture is brought closer to the STR to enable a larger Δf to be used so that less simulation points are required. The simulated bandwidth is 84MHz between 40MHz-124MHz.

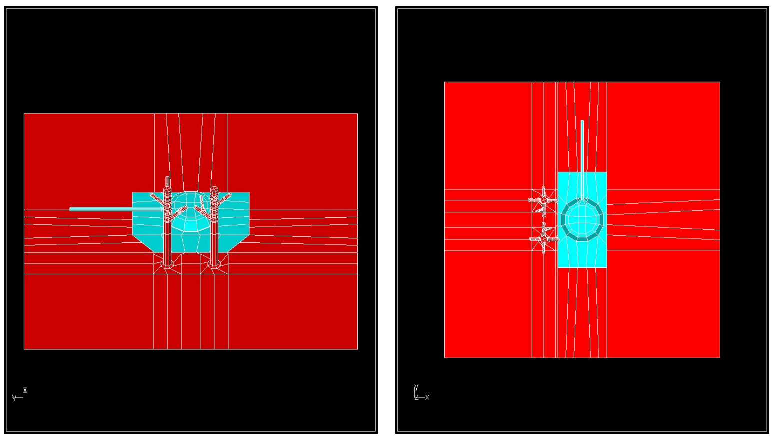

Figure 6: A practical FOPEN scene featuring a tank with dielectric trees and ground plane.

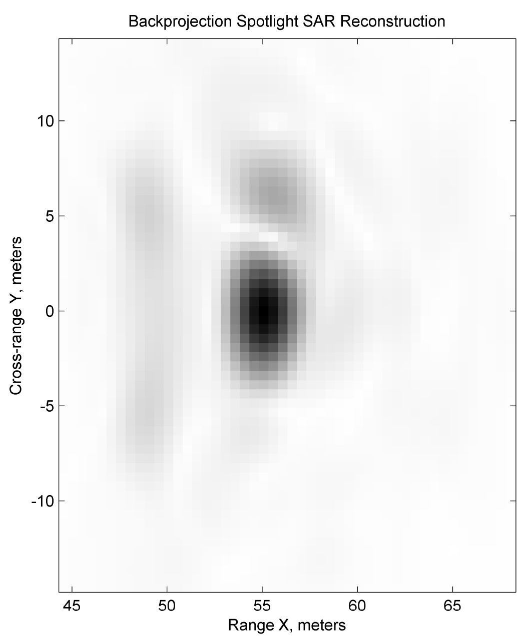

Figure 7: Practical FOPEN scene backprojection spotlight SAR $E_{\varphi\varphi}$ reconstruction

The backprojection spotlight SAR reconstruction for this scene is shown in Figure 7. Although the image resolution is low due to the reduced bandwidth used, a dark area localized around the tank position can still be identified. The presence of the dielectric trees has little observable affect on the reconstruction as a result of the frequency range employed. That is, the radar signal is largely penetrating the foliage at these frequencies. The reconstruction over a larger frequency bandwidth would increase the image resolution but the effect of the foliage would become increasingly apparent. Simulating over a larger bandwidth than this would require a prohibitive amount of time for a single processor analysis. The usage of multiple processors in parallel would remove this limitation.

IV. CONCLUSIONS

This paper has demonstrated the use of numerical electromagnetic analysis for the simulation of low frequency SAR scenes involving various types of targets. Target scenes that included combined metal and dielectric targets to emulate FOPEN type scenarios were demonstrated as well. The reconstructed metal targets are at the correct range location and have approximately the correct cross-range dimension. Of particular interest are the preliminary results demonstrating basic FOPEN scene generation. The ability to analyze and predict the distortion of target signatures under various conditions of concealment will be a significant application of this approach. The generation of larger, more complex FOPEN scenes using multiple processors is currently being investigated. The results presented here show that a numerical electromagnetic approach based on the method of moments can indeed be used to for FOPEN SAR imaging applications.

The practical FOPEN example presented here could not be simulated over a larger frequency range to enable the analysis of reconstruction at higher frequencies. Given the limitations of the available computing platforms, the frequency range for this example is the largest that could be analyzed in any reasonable length of time. The development of a practical FOPEN SAR simulator requires significant advances in computational power and software written so that the computational load can be distributed over multiple processors.

ACKNOWLEDGMENTS

This effort was supported by a research contract with Black River Systems Corp., Utica, NY as a sub-contract on contract F30602-01-C-0203 with the Air Force Research Laboratory, Rome, NY.

REFERENCES

[1] Ward, J., *Space-time adaptive processing for airborne radar*. 1994, MIT Lincoln Laboratory: Cambridge, MA.

[2] Harrington, R.F., *Field Computation by Moment Methods*. 1982: Robert E. Kreiger Publishing Co.

[3] Kolundzija, B.M., B.D. Popovic, *Entire-domain Galerkin method for analysis of metallic antennas and scatterers*. Proceedings of the IEE, Part H, 1992. 140(1):p. 1-10.

[4] Kolundzija, B.M., B.D. Popovic, T.K. Sarkar, R.F. Harrington, *WIPL-D Professional Version*. 2000, OHRN Enterprises: Dewitt, NY.

[5] Soumekh, B., *Synthetic Aperture Radar Signal Processing with MATLAB Algorithms*. 1999, New York: John Wiley.

[6] Knott, E.F., Shaeffer, J.F., Tuley, M.T., *Radar Cross Section*. 1993, Artech House.

[7] Simcoe, M., Chen, E., Adve, R., Qureshi, F., Schneible, J., Wicks, M., *FOPEN Scene Generation Using Numerical Electromagnetic Analysis*. IEEE Conference on Radar, 2003. p. 362-369.

